Influence of the atomic-scale structure on the exciton fine-structure splitting in InGaAs and GaAs quantum dots in a vertical electric field

Jun-Wei Luo, Ranber Singh, Alex Zunger, and Gabriel Bester

Phys. Rev. B **86**, 161302 — Published 10 October 2012

DOI: 10.1103/PhysRevB.86.161302

Influence of the atomic-scale structure on the exciton fine-structure splitting in InGaAs and GaAs quantum dots in a vertical electric field

Jun-Wei Luo,[1] Ranber Singh,[2] Alex Zunger,[3] and Gabriel Bester[2]

[1] *National Renewable Energy Laboratory, Golden, Colorado 80401, USA*
[2] *Max-Planck-Institut für Festkörperforschung, Heisenbergstrasse 1, D-70569 Stuttgart, Germany.*
[3] *University of Colorado, Boulder, Colorado 80309, USA*

(Dated: September 14, 2012)

We investigate the vertical electric field tuning of the exciton fine structure splitting (FSS) in several InGaAs and GaAs quantum dots (QDs) using the atomistic empirical pseudopotential approach and configuration interaction. We find that the FSS is surprisingly tunable, with a rate similar to the one reported for lateral electric fields. The minimum FSS for GaAs QDs often lies below the radiative linewidth, which makes them good candidates for the generation of entangled photon pairs. We highlight, however, that random alloy fluctuations affect the minimum FSS by $\pm$ 1.4 μeV, so that a post-selection of QDs may still be beneficial to obtain entangled photon pairs with the highest fidelity. We suggest a simple experimental procedure for this task. The FSS is therefore a rare observable, where the specific decoration of the random alloy lattice, significantly matters.

PACS numbers: 78.67.Hc,73.21.La, 03.67.Bg,42.50.Dv

One of the leading proposals for *on demand* generation of polarization entangled photons is the utilization of the cascade decay of biexciton-exciton-ground state[1] in semiconductor quantum dots (QDs)[2] as illustrated schematically in Fig. 1a. A serious impediment to the success of this proposal is the existence of a natural splitting within the single exciton manifold (Fig. 1a) called "fine structure splitting" (FSS) that must be suppressed below the radiative linewidth ($\approx$ 1 μeV). The FSS is affected by the atomistic symmetry of the QD confining potentials[3–8] and can be manipulated by strain[9,10], lateral electric fields[11], vertical electric fields[12–14], magnetic field[15] and strong coherent lasers[16,17]. A number of surprising puzzles surround the tuning of the FSS by a vertical electric field. First, it is predicted theoretically[18], and confirmed experimentally[10,13] and theoretically[19], that for QDs made of random alloys (with symmetry lower than C_{2v}) the two bright components of the excitons undergo an *anticrossing* as a function of fields applied along the {100} or {110} directions[18]. Second, since it has been established that the FSS is related to the atomistic in-plane asymmetry between the [110] and [1$\bar{1}$0] crystallographic directions, it would appear that such an intrinsic quantity would not lend itself to tuning via *vertical* field. Nevertheless, it was shown experimentally that the FSS can be tuned rather effectively in In(Ga)As/GaAs QDs by applying an electric field along the growth direction[13]. Third, the role of strain is unclear: while electric field control was observed in strain-free monolayer thickness fluctuation GaAs QDs[12,14], investigations of this effect for other strain-free GaAs QDs grown by multi-step hierarchical self-assembly[20] or droplet epitaxy[21], have not yet been reported. Finally, even though strain-free GaAs/AlGaAs QDs naturally lack the built-in strain asymmetry that was believed to contribute to FSS in strained InAs/GaAs QDs[22], still significant FSS can exist, casting doubt on our understanding of the role of strain in creating FSS-promoting asymmetries in the potential.

Here, we clarify the physical process underlying the tuning of the FSS by vertical electric fields by developing a simple mesoscopic model that allows us to analyze our million atom calculations of a large set of InGaAs/GaAs and GaAs/AlGaAs QDs. We find good agreement of our results for InGaAs QDs with existing experiments[13] and predict that the FSS in strain-free GaAs/AlGaAs QDs is tunable well below the radiative linewidth ($\approx$1 μeV). However, we show that different decorations of the cation lattice in the AlGaAs alloy barrier leads to fluctuations in the minimum FSS in the range of $\pm$ 1.4 μeV, making a post-selection of appropriate QDs necessary. We show that measurements of the FSS and the polarization angle at zero field suffice to identify appropriate QDs.

We consider lens-shaped and Gaussian shaped QDs with sizes, composition and material as given in Table I. The atom positions are relaxed using the valence force field method[23]. The single particle states are calculated using the atomistic empirical pseudopotential approach[23,24], taking strain, band coupling, coupling between different parts of the Brillouin zone and spin-orbit coupling into account, for multi-million atom structures. We apply an external electric field following Ref. 25. The direct and exchange Coulomb interactions are calculated from the atomic wave functions as shown in Ref. 6, and the correlated excitonic states are calculated by the configuration interaction (CI) approach[26] using 12 electron and 12 hole states (spin included), thus accounting for correlations.

Before we present our numerical results, we introduce a mesoscopic simple model where the Hamiltonian is split into different components:

$$H = H_{C2v} + \delta H_{C1} + q_s F z \quad , \tag{1}$$

where q_s is the charge of a particle in band s, i.e. $-e(+e)$

TABLE I: Sizes and compositions of different QDs investigated in this paper. The sizes a, b and h describe the elliptic axis along the [110] and [1$\bar{1}$0] directions and the height, respectively.

QD	composition	size (nm) a ,b, h	barrier (% Al) top	barrier (% Al) bottom
		Lens Shape		
00	$In_{0.8}Ga_{0.2}As$	10, 7.5, 2.5	0	0
01	GaAs	45, 45, 3	35	35
02	GaAs	70, 50, 3	45	45
03	GaAs	70, 50, 3	35	45
04	GaAs	60, 40, 2	35	45
05	GaAs	25, 31, 3.9	35	35
		Gaussian Shape		
06	GaAs	30, 30, 3	30	30
07	GaAs	30, 30, 4	30	30
08	GaAs	30, 30, 6	30	30
09	GaAs	35, 30, 3	30	30
10	GaAs	35, 30, 4	30	30
11	GaAs	35, 30, 6	30	30
12	$Al_{0.06}Ga_{0.94}As$	30, 30, 3	30	30
13	$Al_{0.06}Ga_{0.94}As$	30, 30, 6	30	30
14	$Al_{0.06}Ga_{0.94}As$	35, 30, 3	30	30
15	$Al_{0.06}Ga_{0.94}As$	35, 30, 6	30	30

for conduction (valence) bands, H_{C2v} is the Hamiltonian of the QD with C_{2v} point group symmetry, which must be supplemented by the deviation from this symmetry by the term δH_{C1}. This latter term represents the random alloy present in the barrier and possible impurities inside the GaAs QD, as well as shape asymmetries. In the space of the two bright states $|1\rangle$ and $|2\rangle$ the Hamiltonian has a simple form:

$$H = \begin{pmatrix} E_1 + \delta E_1 + \gamma_1 F & s_0/2 \\ s_0/2 & E_2 + \delta E_2 + \gamma_2 F \end{pmatrix} \quad . \qquad (2)$$

The exciton energies of the high symmetric hypothetical structure given by $E_1 = \langle 1|H_{C2v}|1\rangle$ and $E_2 = \langle 2|H_{C2v}|2\rangle$ are different due mainly to strain[22] (nearly vanishing in the case of strain free GaAs QDs). The lowering of the symmetry to C_1 leads to the terms $\delta E_1 = \langle 1|\delta H_{C1}|1\rangle$ and $\delta E_2 = \langle 2|\delta H_{C1}|2\rangle$ and also to $s_0/2 = \langle 1|\delta H_{C1}|2\rangle$ and $\gamma_i = \langle i|q_s z|i\rangle$. Redefining $E_1 + \delta E_1$ as E_0 and $\delta = E_2 - E_1 + \delta E_2 - \delta E_1$ and removing the linear term in the field from $|1\rangle$ leads to

$$H = \begin{pmatrix} E_0 & s_0/2 \\ s_0/2 & E_0 + \delta + (\gamma_2 - \gamma_1)F \end{pmatrix} \quad , \qquad (3)$$

which corresponds to the anticrossing model used by Bennett *et al.*[13]:

$$E \begin{pmatrix} \cos\theta \\ \sin\theta \end{pmatrix} = \begin{pmatrix} E_0 & s_0/2 \\ s_0/2 & E_0 - \gamma(F - F_0) \end{pmatrix} \begin{pmatrix} \cos\theta \\ \sin\theta \end{pmatrix} \quad . \qquad (4)$$

We identify $\gamma = \gamma_1 - \gamma_2$ and $\gamma F_0 = \delta$ from Eqs.(2) and (4). This simple reformulation clarifies the origin of the terms. γ being the difference in the response of $|1\rangle$ and $|2\rangle$ to the applied field and γF_0 being the intrinsic FSS due to the inequivalence of [110] and [1$\bar{1}$0] in C_{2v} (small for a strain free structure) and the lowering to C_1 symmetry through atomistic alloy effects. s_0 is the FSS at the anticrossing and quantifies the coupling between the bright states. In a pure GaAs QD embedded in a pure AlAs matrix the bright states are expected to cross[18] due to the high C_{2v} symmetry of the structure and $s_0 = 0$. However, the reduction of the QD symmetry due to the alloy fluctuations in the AlGaAs barrier at the QD interface leads to an avoided crossing[18] with $s_0/2 \neq 0$. F_0 is the field at the anticrossing. As the field approaches F_0 the exciton eigenstates become a coherent mixture with components $\sin\theta$ and $\cos\theta$, where θ is the angle describing the orientation of the lowest eigenstate relative to the [110] crystal axis. The solution of Eq.(4) yields the eigenvalues ($E_\pm$) and angles[13]:

$$E_\pm = E_0 - \frac{\gamma(F - F_0)}{2} \pm \frac{1}{2}\sqrt{\gamma^2(F - F_0)^2 + s_0^2} \qquad (5)$$

$$\theta = \pm \tan^{-1}\left[\frac{s_0}{\gamma(F - F_0) \pm (E_- - E_+)}\right] \quad . \qquad (6)$$

We note at this point, that the model of Eq. (2) does not include any field dependence of the off-diagonal terms. Such terms would lead to an additional coupling of the two bright states and could be used to tune the FSS through zero (if it would exactly compensate $s_0/2$). In our case of vertical field, this coupling is negligible, but in the case of a field with a component along a low symmetry direction (any direction but [110] or [1$\bar{1}$0]) this term should exist. A future investigation of this effect would be worthwhile.

We first present our results for the strained $In_{0.8}Ga_{0.2}As$ QD00 (see Table I) an emission energy that fits the measured results of Bennett *et al.*[13] very well. Figure 1 shows the Stark shift, FSS and the oscillator strength as a function of vertical electric field. We obtain a nearly linear change in the FSS with the E-field in agreement with the experimental results[13]. A fit of our numerical results to the model of Eq.(4) yields the parameters given in Table II. For the field dependence of the FSS, γ, we obtain a value of 0.15 μeV cm/kV, somewhat lower than the value of 0.28 μeV cm/kV reported by Bennett *et al.*[13]. The strong shape and size dependence of the slope can explain this discrepancy and will be illustrated below. Our results for the set of strain-free GaAs QDs given in Table I are shown in Fig. 2 and 3, where we plotted the Stark shift, the FSSs, the polarization angle θ and the oscillator strength as a function of the vertical E-field. The results of the fit to the model of Eq.(4) are given in Table II. We make the following observations.

FSS and polarization angle: The anticrossing described by Eq. (4) can be seen in Figs. 2c) and Fig. 3 as a reduction of the FSS until the value s_0, followed by an increase. The anticrossing is accompanied by a rotation of the polarization angle of the lowest energy exciton state[18], as shown in Fig. 2a). At the field F_0, where the anticrossing

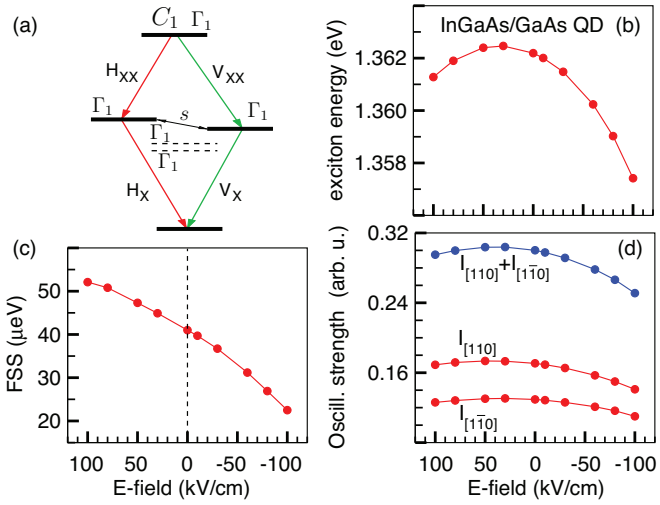

FIG. 1: (a) Schematic representation of the biexciton → exciton → ground-state cascade. (b) Exciton energy, (c) FSS, (d) oscillator strength of the bright exciton transitions along the [110] and [1$\bar{1}$0] directions as a function of applied electric field for the strained InGaAs/GaAs QD00 (see table I).

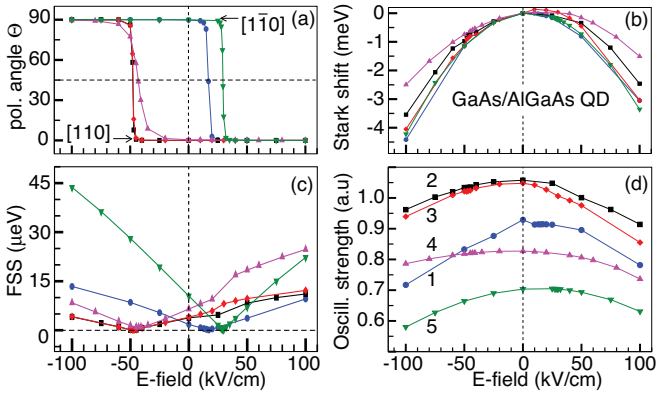

FIG. 2: Results for GaAs/AlGaAs strain free QDs. (a) Polarization angle θ, (b) Stark shift, (c) FSS, (d) Sum of intensities along the [110] and the [1$\bar{1}$0] crystal directions as a function of applied vertical E-field. The circles, squares, diamonds, up-triangles and down-triangles are for the QD01, QD02, QD03, QD04 and QD05, respectively.

occurs, the polarization angle changes more rapidly when s_0 is small; in agreement with the model.

Shape and size effects on the tunability γ: Table II reveals that γ increases with the height of the QDs: tall dots are more tunable in the vertical electric field, which correlated with the polarizability of the exciton states. Comparing QD05 and QD07 with similar dimensions but different shapes, shows that Gaussian shaped dots have a larger γ value.

Shape and size effects on s_0: From Table II we conclude that the shape effect on s_0 is rather moderate, while the size effect shows a trend for larger values of s_0 in larger QDs. This latter trend is, however, overshadowed by a

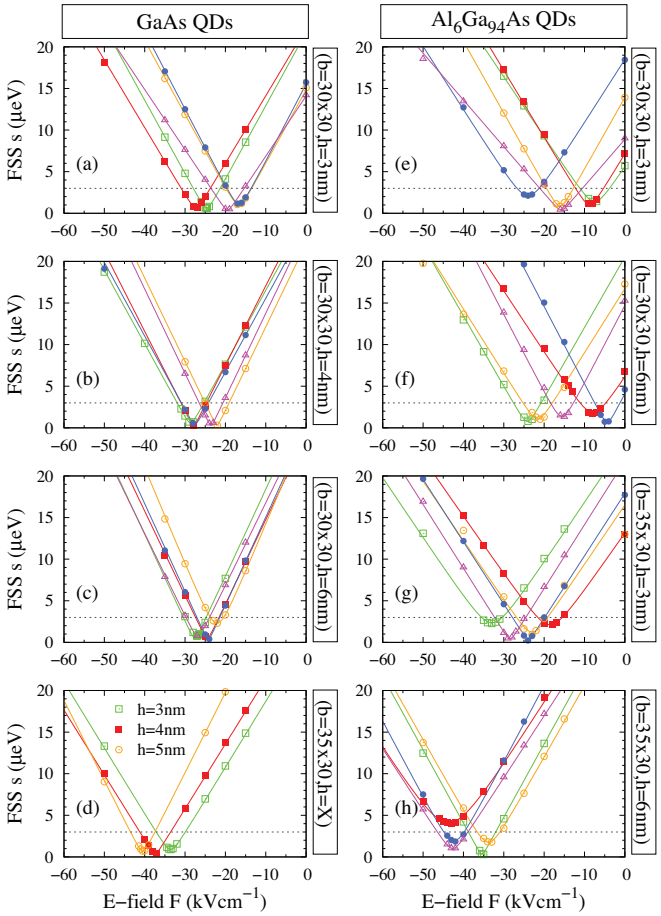

FIG. 3: FSS as a function of the electric field for various QDs listed in Table I. Five different alloy configurations of the $Al_{30}Ga_{70}As$ matrix have been used in (a)-(c), and five different QD alloy configurations in (e)-(h).

very strong random alloy effect (see next).

Random alloy effects on s_0 and F_0: In Fig. 3a-c) we generated the same QD structure with different random realizations of the barrier material. In Fig. 3e-g) the QDs have a 6% Al content and these Al atoms are randomly distributed in 5 different realizations within the QDs. These variations represent fluctuations that should be encountered experimentally. We notice that both s_0 and F_0 are significantly affected by these atomistic effects. For instance, the pure GaAs QD QD08 can exist with s_0 of 0.1 μeV or 1.7 μeV by merely changing the realization (i.e., the random distribution of the cations) of the barrier material. Furthermore, QD15 can exist with s_0 of 0.4 μeV or 3.2 μeV by changing the random distribution of the 6%Al atoms inside the QD. The sensitivity of s_0 and F_0 on the alloy realization is in agreement with our model (Eq. 2), where these terms have been shown to originate from the lowering of the symmetry (term δH_{C1}).

Random alloy effect on γ: The value of γ is only weakly dependent on the details of the alloy realization (see Fig. 3) but rather strongly on the QDs geometry,

TABLE II: Transition energy E_0 and FSS parameters defined in Eq. (4) and extracted from our numerical results. The error bars represent the range of parameters we obtain by running five different random alloy realization (see Fig. 3).

QD	E_0 (meV)	s_0 (μeV)	γ (μeV·cm/kV)	F_0 (kV/cm)
00	1363	?	0.15	+273
01	1644	0.1	0.11	+17
02	1650	0.1	0.08	-48
03	1643	0.1	0.08	-48
04	1742	0.9	0.14	-43
05	1679	0.3	0.33	+29
06	1762 ± 2	0.8 ± 0.3	0.85 ± 0.08	-21 ± 5
07	1718 ± 2	0.4 ± 0.1	0.95 ± 0.06	-26 ± 3
08	1666 ± 1	0.9 ± 0.8	1.06 ± 0.07	-25 ± 2
09	1754	0.9	0.79	-33.5
10	1714	0.4	0.78	-37.4
11	1660	0.7	0.96	-40.5
12	1806 ± 5	1.2 ± 0.7	0.74 ± 0.11	-14 ± 7
13	1727 ± 2	1.2 ± 0.5	0.85 ± 0.09	-15 ± 9
14	1799 ± 2	1.3 ± 1.0	0.73 ± 0.03	-25 ± 6
15	1721 ± 2	1.8 ± 1.4	0.84 ± 0.07	-40 ± 5

size and composition (see Fig. 2c). Indeed, following our model, γ gives the difference in the response of $|1\rangle$ and $|2\rangle$ to the applied field and is directly related to the light-hole component of the exciton state. For a pure heavy-hole exciton, γ vanishes. The light-hole component does change significantly for different shapes (QD01, QD02, QD03, QD04, QD05 have 3.5%, 2.4%, 2.6%, 5.0%, 8.2%, light-hole component, respectively) but remains constant for different alloy realizations.

Oscillator strength: Fig. 2d) shows a moderate change of the oscillator strength, in the range of 10%, with varying E-field in the range of -100 kV/cm to +100 kV/cm.

How to select QDs with small s_0: Our present work shows that GaAs QDs are good candidates to achieve small FSS via vertical electric field, but also that rather large fluctuations of s_0 should be expected within one homogenous set of QDs (that differ only by random alloy effects and have the same shape, size and composition). A selection of appropriate QDs (as practiced experimentally[27,28]) will therefore be advantageous, if not necessary. From Eqs. (5) and (6) at zero field (F=0) we can derive the following expressions:

$$F_0 = \frac{\Delta E \cos 2\theta}{\gamma} \quad ; \quad s_0 = -\Delta E \sin 2\theta \quad , \qquad (7)$$

where ΔE is the FSS at $F = 0$. Interestingly, s_0 does not depend on the slope γ and only requires a single measurement of the FSS and the corresponding polarization angle θ at zero field. We have used Eq.(7) in Table II to report our value of F_0 for QD00. For the value of s_0, however, if ΔE is large, a small inaccuracy in the measurement, or the calculation in our case, of the angle θ will lead to an inaccurate determination of s_0. With a ΔE of 50 μeV and an angle accuracy of 2° we obtain s_0 with an error bar of ± 3.5 μeV, which is too large to be useful. However, Eq.(7) is very useful for QDs where ΔE is not too large, which represent the QDs that will require weaker E-fields to be tuned.

In summary, we showed that the FSS in GaAs/AlGaAs and InGaAs/GaAs self-assembled QDs can be effectively tuned by a vertical electric field. Indeed, the tuning rate for GaAs QDs is between 0.1 and 1 μeV cm/kV, depending on size and geometry, and is surprisingly similar to the tuning rate obtained with lateral electric fields (0.15 μeV cm/kV[29]). Our results for InGaAs QDs are in good agreement with experiment, while the results for GaAs QDs represent predictions. The minimum FSS, s_0, for GaAs QDs, is between 0.1 and 1.8 μeV, depending on size and geometry. However, alloy fluctuations in the surrounding barrier lead to a variations of s_0 in the range of ±1.4 μeV calling for a post-selection of the "best QDs", for which we suggest a simple experimental procedure requiring only one measurement at zero field.

This dependence of s_0, and also F_0, on the random atomic arrangement is in agreement with the expectations from a simple mesoscopic model that shows these terms to be proportional to the "amount of deviation from C_{2v}" symmetry towards the lower C_1 symmetry. Hence, a QD made of a random alloy (with formally C_1 symmetry) with an atomic decoration of the lattice that will *resemble* the C_{2v} symmetry, will have the smallest s_0. This represents a striking example of an observable, where the conventional treatment of a random alloy through a replacement of the atomic distribution by an average (VCA[30]) or an effective medium (CPA[30]), fails. In this case, the position of each and every atom in a structure made of several thousand atoms is relevant.

Acknowledgments

GB and RS would like to acknowledge financial support by the BMBF (QuaHL-Rep, Contract No. 01BQ1034).

[1] O. Benson, C. Santori, M. Pelton, and Y. Yamamoto, Phys. Rev. Lett. **84**, 2513 (2000).
[2] P. Michler, ed., *Single Semiconductor Quantum Dots Series: NanoScience and Technology* (Springer, Berlin, 2009).
[3] M. Bayer, A. Kuther, A. Forchel, A. Gorbunov, V. B. Timofeev, F. Schäfer, J. P. Reithmaier, T. L. Reinecke, and S. N. Walck, Phys. Rev. Lett. **82**, 1748 (1999).

[4] R. J. Warburton, C. Schaflein, D. Haft, F. Bickel, A. Lorke, K. Karrai, J. M. Garcia, and P. M. Petroff, Nature **405**, 926 (2000).

[5] T. Takagahara, Phys. Rev. B **62**, 16840 (2000).

[6] G. Bester, S. Nair, and A. Zunger, Phys. Rev. B **67**, 161306(R) (2003).

[7] L. Besombes, K. Kheng, and D. Martrou, Phys. Rev. Lett. **85**, 425 (2000).

[8] R. Seguin, A. Schliwa, S. Rodt, K. Potschke, U. W. Pohl, and D. Bimberg, Phys. Rev. Lett. **95**, 257402 (2005).

[9] S. Seidl, M. Kroner, A. Hogele, K. Karrai, R. Warburton, A. Badolato, and P. Petroff, Appl. Phys. Lett. **88**, 203113 (2006).

[10] J. Plumhof, V. Křápek, F. Ding, K. Jöns, R. Hafenbrak, P. Klenovský, A. Herklotz, K. Dörr, P. Michler, A. Rastelli, et al., Phys. Rev. B **83**, 121302 (2011).

[11] K. Kowalik, O. Krebs, A. Lemaitre, S. Laurent, P. Senellart, P. Voisin, and J. A. Gaj, Appl. Phys. Lett. **86**, 041907 (2005).

[12] S. Marcet, K. Ohtani, and H. Ohno, Appl. Phys. Lett. **96**, 101117 (2010).

[13] A. J. Bennett, M. A. Pooley, R. M. Stevenson, M. B. Ward, R. B. Patel, A. B. d. l. Giroday, N. Sköld, I. Farrer, C. A. Nicoll, D. A. Ritchie, et al., Nature Phys. **6**, 947 (2010).

[14] M. Ghali, K. Ohtani, Y. Ohno, and H. Ohno, Nature Communications **3**, 661 (2012).

[15] R. Stevenson, R. Young, P. Atkinson, K. Cooper, D. Ritchie, and A. Shields, Nature **439**, 179 (2006).

[16] G. Jundt, L. Robledo, A. Hogele, S. Fält, and A. Imamoglu, Phys. Rev. Lett. **100** 177401(2008).

[17] A. Muller, W. Fang, J. Lawall, and G. S. Solomon, Phys. Rev. Lett. **103** 217402(2009).

[18] R. Singh and G. Bester, Phys. Rev. Lett. **104**, 196803 (2010).

[19] M. Gong, W. Zhang, G.-C. Guo, and L. He, Phys. Rev. Lett. **106**, 227401 (2011).

[20] A. Rastelli, S. Stufler, A. Schliwa, R. Songmuang, C. Manzano, G. Costantini, K. Kern, A. Zrenner, D. Bimberg, and O. Schmidt, Phys. Rev. Lett. **92**, 166104 (2004).

[21] K. Watanabe, N. Koguchi, and Y. Gotoh, Jpn. J. Appl. Phys. **39**, L79 (2000).

[22] G. Bester and A. Zunger, Phys. Rev. B **71**, 045318 (2005).

[23] A. J. Williamson, L.-W. Wang, and A. Zunger, Phys. Rev. B **62**, 12963 (2000).

[24] L.-W. Wang and A. Zunger, Phys. Rev. B **59**, 15806 (1999).

[25] G. Bester and A. Zunger, Phys. Rev. B **72**, 165334 (2005).

[26] A. Franceschetti, H. Fu, L.-W. Wang, and A. Zunger, Phys. Rev. B **60**, 1819 (1999).

[27] R. J. Young, R. M. Stevenson, A. J. Shields, P. Atkinson, K. Cooper, D. A. Ritchie, K. M. Groom, A. I. Tartakovskii, and M. S. Skolnick, Phys. Rev. B **72**, 113305 (2005).

[28] R. M. Stevenson, C. L. Salter, J. Nilsson, A. J. Bennett, M. B. Ward, I. Farrer, D. A. Ritchie, and A. J. Shields, Phys. Rev. Lett. **108**, 040503 (2012).

[29] M. M. Vogel, S. M. Ulrich, R. Hafenbrak, P. Michler, L. Wang, A. Rastelli, and O. G. Schmidt, Appl. Phys. Lett. **91**, 051904 (2007).

[30] M. Jaros, Rep. Prog. Phys. **48**, 1091 (1985).